Mobility induces global synchronization of oscillators in periodic extended systems

2010 New J. Phys. 12 093029

(http://iopscience.iop.org/1367-2630/12/9/093029)

New Journal of Physics
The open-access journal for physics

Mobility induces global synchronization of oscillators in periodic extended systems

Fernando Peruani[1,2], **Ernesto M Nicola**[2,3] **and Luis G Morelli**[2,4,5]

[1] CEA-Service de Physique de l'Etat Condensé, Centre d'Etudes de Saclay, 91191 Gif-sur-Yvette, France
[2] Max Planck Institute for the Physics of Complex Systems, Nöthnitzer Str. 38, 01187 Dresden, Germany
[3] IFISC, Institute for Cross-Disciplinary Physics and Complex Systems (CSIC-UIB), Campus Universitat Illes Balears, E-07122 Palma de Mallorca, Spain
[4] Departamento de Física, FCEyN, UBA, Ciudad Universitaria, 1428 Buenos Aires, Argentina
[5] Max Planck Institute of Molecular Cell Biology and Genetics, Pfotenhauerstr. 108, 01307 Dresden, Germany
E-mail: peruani@pks.mpg.de, ernesto.nicola@ifisc.uib-csic.es and morelli@mpi-cbg.de

New Journal of Physics **12** (2010) 093029 (11pp)
Received 12 April 2010
Published 17 September 2010
Online at http://www.njp.org/
doi:10.1088/1367-2630/12/9/093029

Abstract. We study the synchronization of locally coupled noisy phase oscillators that move diffusively in a one-dimensional ring. Together with the disordered and the globally synchronized states, the system also exhibits wave-like states displaying local order. We use a statistical description valid for a large number of oscillators to show that for any finite system there is a critical mobility above which all wave-like solutions become unstable. Through Langevin simulations, we show that the transition to global synchronization is mediated by a shift in the relative size of attractor basins associated with wave-like states. Mobility disrupts these states and paves the way for the system to attain global synchronization.

Contents

The synchronization of oscillators is a widespread phenomenon in nature [1]–[3]. In biology, synchronization can occur at scales that range from groups of single cells to ensembles of complex organisms [4]. When oscillators hold fixed positions in space and the interaction that drives synchronization is short ranged, spatial and temporal patterns can self-organize. This is the case for cardiac tissue, where cells generate spiral patterns that shape the heartbeats [5]. Also in central pattern generators, the oscillating neural network self-organizes to produce coordinated movements of the body [6].

A different situation arises when the oscillators are not fixed in space but are able to move around. The problem of synchronization of moving oscillators has many applications in the domain of chemistry [7], biology [8] and technology [9]. Small porous particles loaded with the catalyst of the Belousov–Zhabotinsky reaction behave as individual chemical oscillators, undergoing a density-dependent synchronization transition as the stirring rate is increased [7]. The same particles support wave propagation in the form of dynamic target and spiral patterns when the particles are not moving [10]. This phenomenon illustrates a wider scenario: mobility and mixing remove local defects and patterns, enabling global order. This effect has far-reaching consequences in finite systems. For example, in ecosystems of competing populations with cyclic interactions, biodiversity can be sustained if dispersal is local, but it is lost when dispersal occurs over large length scales [11]. The dynamics of such cyclic competition was described by a complex Ginzburg–Landau equation near a Hopf bifurcation, displaying complex oscillatory patterns indicative of biodiversity for low mobility, while in the case of high mobility diversity is wiped out [12, 13].

In this paper, we study the effects of mobility—spatial diffusion—on the macroscopic collective dynamics of locally coupled, moving phase oscillators subjected to noise, in a one-dimensional ring. When oscillators are fixed in space, these systems can exhibit a series of steady states where local order is present [14]–[16]. Such states have been called m-twist solutions [16] (figure 1). Here, we show that mobility can destabilize all m-twist solutions, enhancing the stability of the synchronized solution. We find that in finite systems there is a critical mobility above which either the synchronized or the disordered state is stable.

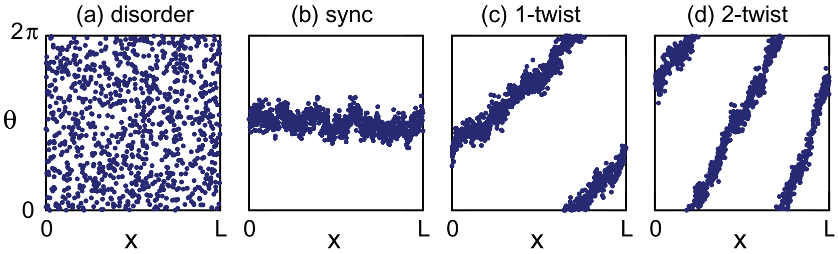

Figure 1. The system, equations (1) and (2), exhibits different kinds of states: (a) disorder, (b) partial synchronization and twisted states, e.g. (c) 1-twist and (d) 2-twist. Each dot (x, θ) represents an oscillator. Parameters in arbitrary units: $N = 1000$, $L = 2\pi$, $r = L/100$, $\omega = 0$, $\gamma = 0.1$ and $\sqrt{2D} = 0.01$. In (a), $\sqrt{2C} = 0.35$, and in (b)–(d), $\sqrt{2C} = 0.10$. States (b)–(d) coexist. The snapshots were taken after 15 000 time units, starting from random initial conditions.

1. Diffusing phase oscillators

We consider an ensemble of N identical phase oscillators that diffuse on a ring of perimeter L. Oscillators are coupled to other oscillators in their local neighborhood, within an interaction range r. The dynamics of phase and position is described by

$$\dot{\theta}_i(t) = \omega - \gamma \left[\frac{1}{n_i} \sum_{|x_i - x_j| < r} \sin(\theta_i - \theta_j) \right] + \sqrt{2C}\xi_{\theta,i}(t), \tag{1}$$

$$\dot{x}_i(t) = \sqrt{2D}\xi_{x,i}(t), \tag{2}$$

where $i = 1, \ldots, N$ is the oscillator label, $\theta_i(t)$ and $x_i(t)$ are the phase and position of the ith oscillator at time t, ω is the autonomous frequency and γ is the coupling strength—whose inverse characterizes the typical relaxation time of the interaction. Each oscillator interacts with its n_i neighbors in the range r through the coupling function in brackets, which defines an attractive interaction towards the local average of the phase.With the definition of the coupling adopted here, the thermodynamic limit is well defined, and the system reduces to the noisy Kuramoto model for $r = L/2$ [17]. The fluctuation terms $\xi_{\theta,i}$ and $\xi_{x,i}$ represent two uncorrelated Gaussian noises such that $\langle \xi_{\theta,i}(t) \rangle = \langle \xi_{x,i}(t) \rangle = 0$ and $\langle \xi_{\theta,i}(t)\xi_{\theta,j}(t') \rangle = \langle \xi_{x,i}(t)\xi_{x,j}(t') \rangle = \delta_{i,j}\delta(t - t')$. The strength of angular fluctuations is determined by the angular diffusion coefficient C, while the spatial diffusion coefficient D determines the mobility of oscillators. The random movement of the oscillators described by equation (2) is not affected by the presence of other oscillators, so in steady state the spatial density is uniform and the number of neighbors is on average constant, $n = n_i = Nr/L$. Both the phase $\theta_i(t)$ and position $x_i(t)$ are periodic variables such that $0 \leqslant \theta_i(t) \leqslant 2\pi$ and $0 \leqslant x_i(t) \leqslant L$.

2. Global order parameter

The system described by equations (1) and (2) displays a range of states illustrated in figure 1. We can characterize global order by the order parameter Z, defined as the absolute

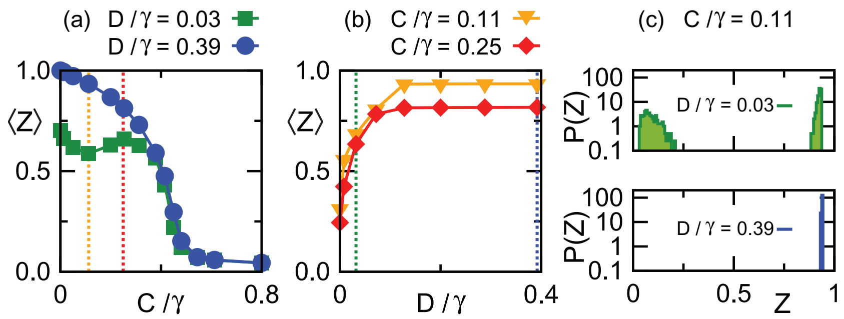

Figure 2. Twisted states affect the ensemble average of the global order parameter, $\langle Z\rangle$. (a) $\langle Z\rangle$ versus scaled angular diffusion C/γ for $D/\gamma = 0.03$ (green squares) and $D/\gamma = 0.39$ (blue dots). For small D/γ, $\langle Z\rangle$ does not reach 1, even for $C = 0$. Vertical dotted lines correspond to the values of C/γ in (b). (b) $\langle Z\rangle$ versus scaled mobility D/γ for $C/\gamma = 0.11$ (orange triangles) and $C/\gamma = 0.25$ (red diamonds). Note that as D is reduced, $\langle Z\rangle$ decays. Vertical dotted lines correspond to the values of C/γ in (a). (c) The histogram of Z splits into two different peaks at low and high values of Z for low values of D/γ, but displays only one peak at high Z for high D/γ. The other parameters are $N = 1000$, $L = 2\pi$, $r/L = 0.01$, $\omega = 0$ and $\gamma = 0.1$.

value of the population average of the complex unit vectors of the oscillator phases $Z(t) = N^{-1}|\sum_j \mathrm{e}^{\mathrm{i}\theta_j(t)}|$ [18]. In figures 2(a) and (b), we plot the ensemble average of the global order parameter $\langle Z\rangle$, computed over 100 different random initial conditions and realizations of the noise. In each individual realization, we measured the value of Z after 5000 time units, corresponding to 5×10^5 integration steps of 0.01 time units. Mobility introduces a dramatic change in the ensemble average of the order parameter $\langle Z\rangle$. When mobility is large enough, the system displays global synchronization as $C \to 0$ (blue dots in figure 2(a)). However, when mobility is reduced, global order is compromised, as indicated by the green squares in figure 2(a). Increasing mobility D results in an increase of the ensemble average $\langle Z\rangle$ (figure 2(b)). The cause for this behavior can be traced back to the existence of twisted states, which display local order but have themselves a vanishing global order parameter (figures 1(c) and (d)). We constructed histograms of the value of the global order parameter Z over 600 different realizations, in which the order parameter was measured after 1000 time units. Due to the presence of twisted states, $\langle Z\rangle$ results from the average of a bimodal distribution $P(Z)$, with a peak related to the twisted states and the other to global synchronization. Above a critical value of the mobility, twisted states are no longer observed and $P(Z)$ becomes unimodal (figure 2(c)). Thus, although a global order parameter is not suited to capture the complexity of a system with local interactions, its statistics reflects the existence of twisted states.

3. Statistical description

The role of twisted states can be studied using a statistical description that is valid when the number of oscillators is large. Given that the oscillators have identical autonomous frequencies ω, it is convenient to make the transformation $\theta \to \theta - \omega t$ to a rotating reference frame. We coarse-grain the microscopic model and describe the system in terms of $\rho(x, \theta, t)$, the density of oscillators at position x with phase θ, which obeys the Fokker–Planck equation

$$\partial_t \rho(x,\theta,t) = D\partial_{xx}\rho(x,\theta,t) + C\partial_{\theta\theta}\rho(x,\theta,t) + \frac{\gamma}{n(x)}\partial_\theta\left[\int_0^L \mathrm{d}x' \int_0^{2\pi} \mathrm{d}\theta' g(x-x')\sin(\theta-\theta')\rho(x',\theta',t)\rho(x,\theta,t)\right], \tag{3}$$

where $g(x-x')$ is a kernel accounting for the range and relative strength of local interactions, while

$$n(x) = \int_0^L \mathrm{d}x' \int_0^{2\pi} \mathrm{d}\theta' g(x-x')\rho(x',\theta',t)$$

denotes the effective number of oscillators in this range. In this paper, we choose $g(x-x') = 1$ for $|x-x'| < r$ and $g(x-x') = 0$ otherwise, as in equation (1). The derivation of equation (3) relies on the assumption that $\rho_2(x,\theta,t;x',\theta',t) = \rho(x,\theta,t)\rho(x',\theta',t)$ [19].

Since the movement of the oscillators is purely diffusive, see equation (2), the spatial density of the oscillators is uniform in steady state, $\int_0^{2\pi} \mathrm{d}\theta\rho(x,\theta,t) = N/L \equiv \rho_0$, and $n(x) = 2r\rho_0$. For small N, fluctuations in the spatial density can induce the formation of gaps in which the nearest oscillator is beyond the range of interaction. In this paper, we consider large densities such that the lifetime of these gaps is much shorter than other typical timescales.

3.1. Local order parameter

The statistical description (3) can be cast in a more transparent form by introducing a local mean field. Local order can be characterized by a local order parameter [14, 15]

$$R(x,t)\mathrm{e}^{\mathrm{i}\psi(x,t)} = \int_0^L \mathrm{d}x \int_0^{2\pi} \mathrm{d}\theta' \frac{g(x-x')}{n(x)} \mathrm{e}^{\mathrm{i}\theta'}\rho(x',\theta',t), \tag{4}$$

where $R(x,t)$ is a measure of local order and $\psi(x,t)$ is the local average of the phase. Equation (3) can be expressed in terms of this local order parameter as

$$\partial_t\rho(x,\theta,t) = D\partial_{xx}\rho(x,\theta,t) + C\partial_{\theta\theta}\rho(x,\theta,t) + \gamma R(x,t)\partial_\theta(\sin(\theta-\psi(x,t))\rho(x,\theta,t)), \tag{5}$$

reflecting the fact that $\psi(x,t)$ acts as a local mean field and $R(x,t)$ is a local modulation to the coupling strength.

4. Transition from disorder to local order

Equation (3) has a trivial steady state $\rho(x,\theta,t) = \rho_0/2\pi \equiv \rho_\mathrm{d}$ that corresponds to the disordered state of the system. We study the stability of ρ_d by inserting $\rho(x,\theta,t) = \rho_\mathrm{d} + \epsilon f(x,t)\cos(\ell\theta)$ in equation (3) and keeping terms of order $O(\epsilon)$ [20]. Linear stability analysis reveals that the disordered solution ρ_d becomes unstable for $\ell = 1$ when the angular diffusion is such that $C < C^*$, with

$$C^* = \gamma/2. \tag{6}$$

This threshold is independent of ρ_0 and D, and determines the value of C below which local order sets in. The critical C^* given by equation (6) coincides with the existence [17] and stability [20] threshold displayed by globally coupled noisy oscillators.

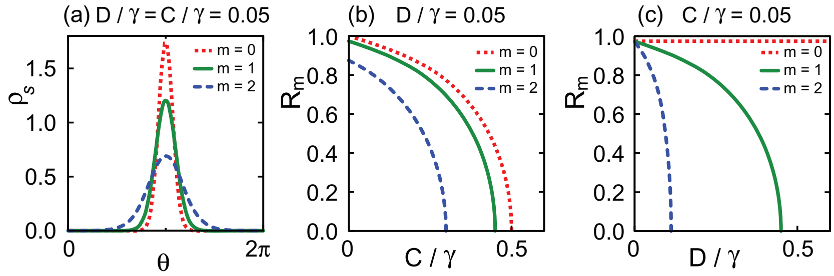

Figure 3. Twisted solutions and local order. (a) Angular distribution of steady-state twisted solutions, equation (8). (b) The local order parameter R_m decreases with increasing angular fluctuations for all solutions, equation (12). (c) The local order parameter of twisted solutions also decreases with mobility, but global order is not affected, equation (12). The range of interaction is $r/L = 0.01$.

5. Local order solutions

Once local order has set in, the system also supports twisted solutions. We specifically look for steady state-solutions to equation (5) of the form $\rho_s(x,\theta) = f(\theta - \psi(x))$. Such wave-like solutions describe densities in which the angular distribution has the same shape but is centered at position-dependent phases $\psi(x)$. Setting $\partial_t \rho = 0$, we obtain an ordinary differential equation for f,

$$\left(C + D\left(\psi'(x)\right)^2\right) f'(\varphi) + \left(\gamma R(x)\sin(\varphi) - D\psi''(x)\right) f(\varphi) = W(x), \tag{7}$$

which we can solve together with periodic boundary conditions in phase and space. We select solutions with $\psi''(x) \equiv 0$, corresponding to the twisted states observed in numerical simulations (figures 1(c) and (d)). These solutions display spatially uniform local order, $R(x) = R$. Periodicity of the phase then implies $W(x) = 0$, and periodicity of space sets the wave numbers $k = 2\pi m/L$ with m being an integer. We obtain the m-twist steady-state solutions

$$\rho_s(x,\theta) = \mathcal{N} \exp\left[\frac{\gamma R}{\mathcal{D}_{\rm eff}} \cos(\theta - kx)\right], \tag{8}$$

where $\mathcal{N}$ is a normalization constant such that $\int_0^{2\pi} \mathrm{d}\theta \int_0^L \mathrm{d}x \rho_s(x,\theta) = N = L\rho_0$, see figure 3(a). We have introduced the effective diffusion coefficient

$$\mathcal{D}_{\rm eff}(k) = C + k^2 D, \tag{9}$$

which is a combination of angular diffusion C, and mobility D scaled by the square of the wave number k. Effective diffusion competes with the local coupling γR and controls the width of the angular distribution, which has a mean $\langle\theta\rangle = kx$ and variance

$$\sigma^2 = 1 - I_1(\gamma R/\mathcal{D}_{\rm eff})/I_0(\gamma R/\mathcal{D}_{\rm eff}), \tag{10}$$

where

$$I_n(z) = \int_0^{2\pi} \mathrm{d}\theta \cos^n\theta \exp\left(z\cos\theta\right) \tag{11}$$

is the modified nth-order Bessel function of the first kind. The functional form of the steady-state angular distribution equation (8) is known as the circular normal distribution [21].

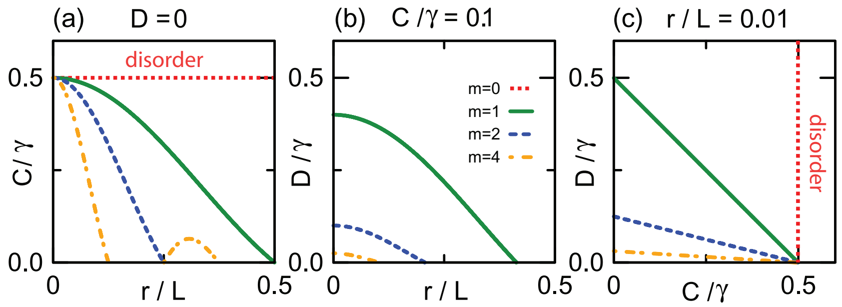

Figure 4. Mobility controls the existence of m-twist solutions. Three representative cuts of the phase diagram are shown for $m = 0, 1, 2$ and 4. (a) $D = 0$, (b) $C/\gamma = 0.1$ and (c) $r/L = 0.01$. The dotted red line indicates the onset of local order, which is independent of D. Below the solid green line, dashed blue line and dot-dashed yellow line, the 1-twist, 2-twist and 4-twist solutions exist, respectively, see equation (14). An increasing number of coexisting twisted solutions can be found with decreasing mobility D and decreasing coupling range r.

5.1. Effective diffusion controls the local order parameter

The m-twist solutions described by equation (8) exist if and only if the self-consistency condition obtained by inserting equation (8) into (4) is fulfilled,

$$R_m = \mathrm{sinc}(kr)\frac{I_1(\gamma R_m/\mathcal{D}_{\mathrm{eff}})}{I_0(\gamma R_m/\mathcal{D}_{\mathrm{eff}})}, \tag{12}$$

where $\mathrm{sinc}(x) = \sin(x)/x$, see figures 3(b) and (c). Using equation (12) in (10) the variance of the distribution can be written as $\sigma^2 = 1 - R_m/\mathrm{sinc}(kr)$. A trivial solution to equation (12) is $R_m = 0$. Apart from this, an expansion of equation (12) for $R_m \ll 1$ reveals that non-vanishing solutions

$$R_m \approx \sqrt{8\mathcal{D}_c\gamma^{-2}}\,(\mathcal{D}_c - \mathcal{D}_{\mathrm{eff}})^{1/2} \tag{13}$$

exist for $\mathcal{D}_{\mathrm{eff}} \leqslant (\gamma/2)\mathrm{sinc}(kr) \equiv \mathcal{D}_c$. Again, we see that $\mathcal{D}_{\mathrm{eff}}$ controls the growth of the local order parameter R_m characterizing the emergence of twisted solutions, through changes in phase fluctuations C and mobility D (figures 3(b) and (c)).

5.2. Existence of twisted solutions

We can unfold the effects of spatial and angular fluctuations by writing $\mathcal{D}_{\mathrm{eff}}$ in terms of its components D and C. Setting $R_m = 0$ in equation (13), we obtain

$$C + (2\pi m/L)^2\, D = (\gamma/2)\mathrm{sinc}\,(2\pi mr/L), \tag{14}$$

where we have expressed k in terms of L to stress system size dependence. For each value of m and range of interaction r, the surface in parameter space defined by equation (14) encloses the region where the m-twist solution exists. There are two ways in which fluctuations can destroy twisted solutions: by increasing either angular fluctuations or mobility. Mobility gets amplified for higher-order modes as m^2, causing twisted solutions to disappear sequentially as mobility increases (figure 4).

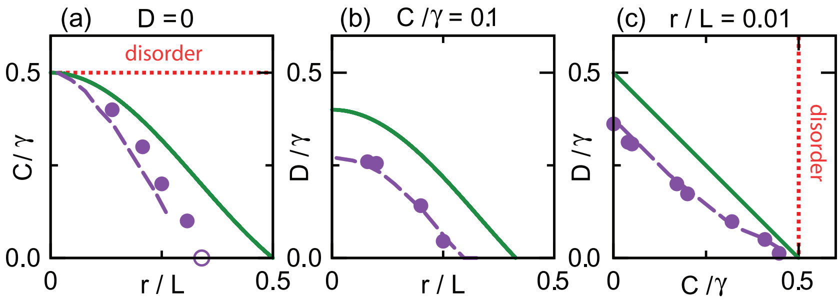

Figure 5. The domains of existence and stability of m-twist solutions do not coincide. The 1-twist solution exists below the solid green line, equation (14), but it becomes stable below the dashed purple line, determined numerically. The purple dots show the stability of the 1-twist state of the Langevin equations (1) and (2). The open circle in (a) corresponds to the limit case $D = C = 0$ studied in [16].

For $m = 0$, equation (14) reduces to $C = C^* = \gamma/2$ and corresponds to global synchronization. The existence of global synchronization in steady state is not affected by mobility, as indicated by the dotted red line in figures 4(a) and (c). However, the existence of twisted solutions in finite systems is controlled by angular diffusion C, mobility D and range of interaction r as indicated by equation (14) (figure 4).

As $L \to \infty$, the critical value of the spatial diffusion coefficient diverges for all m. Therefore, in the infinite system size limit, all twisted solutions coexist with global synchronization for any finite D. This result is in agreement with [22] and indicates that identical noisy phase oscillators cannot exhibit a global synchronized state in 1D in this limit.

5.3. Stability of twisted solutions and states

While existence and stability thresholds coincide for the global order solution, equations (6) and (14), this is not the case for m-twist solutions in finite systems (figure 5). We address the stability of the 1-twist solution by performing a numerical study of equation (3), using a finite difference scheme. To estimate the stability boundary, we continue a stable twist solution until it becomes unstable against small perturbations. We find that the instability is of modulational type. The m-twist solutions become stable only after the corresponding local order parameter R_m becomes larger than a certain value, i.e. twisted solutions become stable with a finite amplitude (figure 5). For vanishing spatial and angular diffusion $C = D = 0$, we encounter the system studied by Wiley *et al* [16], see the purple open circle in figure 5(a). The numerical solution seems to approach this point as $C/\gamma \to 0$, but the numerics become lengthy in this limit.

We next compare the continuum Fokker–Planck description (3) with the discrete system, by means of Langevin simulations of equations (1) and (2). To measure the stability of the 1-twist state in Langevin simulations, we prepare the system in the 1-twist state by randomly positioning the oscillators in space and setting their phase to $\theta(x) = 2\pi x/L$. We first let the system relax for 1000 units of time, so that the stationary shape of the angular distribution is reached. Then, we compute the ensemble average of the twist $\langle m \rangle$, where $\langle \ldots \rangle$ denotes an average over 100 realizations of the numerical simulation, which we performed for different sets of parameter values C, D and r/L. To evaluate the stability of the 1-twist solution, we

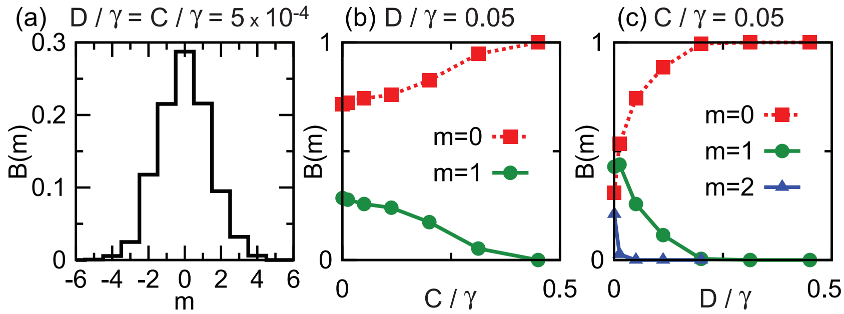

Figure 6. The size of the attraction basins of m-twist solutions depends on the angular fluctuations and mobility. (a) The probability $B(m)$ that, starting from a random initial condition, the system ends up in an m-twist solution. (b, c) $B(0)$ and $B(1)$ as a function of (b) C/γ and (c) D/γ. Parameters are the same as in figure 2.

set a threshold on the average twist: when $\langle m\rangle$ falls below 0.05, we take the 1-twist state to be unstable. Simulations were performed with $N = 1000$ and $L = 2\pi$. Other parameters are indicated in figure 5. The stability threshold in figure 5(a) was found by varying r for various fixed values of C, in figure 5(b) by varying D for fixed values of r and in figure 5(c) by varying C for fixed values of D. We find good agreement between the stability of the 1-twist state of the discrete system and the stability of the 1-twist solution found by numerical integration of the Fokker–Planck equation.

6. Attraction basins

Twisted solutions coexist with global order and among themselves (figure 4). As mobility is increased from low values, twisted solutions become unstable one by one, e.g. figures 4(c) and 5(c), and global order is enhanced, resulting in an increase of the value of the ensemble average of the global order parameter as displayed in figure 2(b). Angular fluctuations can also destabilize twisted solutions (figure 4). However, while increasing the angular fluctuations can decrease the number of twisted solutions competing with global order, the width of the angular distribution corresponding to global order also grows as a consequence of increasing the angular fluctuations. The interplay between these two competing effects may be the cause of the non-monotonic behavior observed in the ensemble average of the global order parameter as angular fluctuations C increase, see green squares in figure 2(a). For these reasons, it is interesting to explore the size of the attraction basins of the different states that the discrete system exhibits.

The fraction of realizations $B(m)$ in which the system ends up in a particular state after a short time, starting from random initial conditions, is a measure of the size of the attraction basins of the state. The coexistence of twisted states with up to $m = 5$ is shown in figure 6(a) for low-mobility and -phase fluctuations, corresponding to the bottom left corner of figure 4(c). As C is decreased, the attraction basin corresponding to global order shrinks, while the attraction basins of the m-twist states expand (figure 6(b)). Decreasing C does not necessarily yield global order at the ensemble level, because the global ordered state shares the phase space with the m-twist solutions: the observed value of $\langle Z\rangle$ results from the competition between an increase in local order for $m = 0$ and a decrease of $B(0)$, see figure 2(a). An increase in the mobility

D leads to a contraction of the attraction basin of the m-twist states, in favor of global order (figure 6(c)). When all m-twist solutions are unstable, $B(0) = 1$, and the global order state is the only attractor below C^*, see also figure 2(b).

7. Discussion

We have investigated the effects of mobility in a generic 1D model of locally coupled moving phase oscillators, and showed that oscillator mobility dramatically affects the collective behavior of finite systems. More specifically, our results show that in low-dimensional systems global synchronization is compromised by the presence of multiple m-twist states exhibiting local order. At the onset of local order, the system can fall into the global synchronized state. However, the coexistence of local order m-twist states implies that the attraction basin of the global synchronization state is reduced. The strong mobility of the oscillators destabilizes these m-twist states and thus promotes global synchronization.

In this paper, we have considered a high density limit such that the connectivity of the system is never interrupted by gaps. In the dilute limit, gaps in the connectivity play a crucial role in the synchronization dynamics. This problem was studied in the context of moving neighborhood networks, and under the assumption of a fast exchange of neighbors, a mean-field condition for the existence and stability of the global synchronization state has been derived [23]. According to this study, whenever the global synchronized state is stable the system reaches global synchronization, regardless of its spatial dimensionality. In other words, the study overlooks the possibility of coexistence of multiple solutions. Our findings reveal a different role for mobility, unrelated to the existence and stability of the global synchronization state: mobility disrupts all these multiple solutions except for the global synchronized state. Extensions of the current study to dilute systems will be further investigated.

Two-dimensional systems display a similar phenomenology, although the competing local order states can now take other forms, e.g. vortexes [24]. It has been recently reported that chaotic oscillators moving in a two-dimensional space can synchronize provided that the spatial dynamics is fast enough [25]. A related albeit different scenario occurs with chaotic advection mixing in two-dimensional systems, where the synchronization of excitable media is enhanced by strong mixing [26, 27]. These results indicate that mobility may also enhance synchronization in two-dimensional systems. We speculate that global synchronization may be achieved by destabilizing local deffects, as we show here for 1D systems. Further work is needed to clarify these issues.

The theoretical framework introduced here may provide insights into other related problems, as when movement is coupled to the oscillator phases. In this case, synchronization can be interpreted as collective motion [28]. As a result of this coupling, strong spatial fluctuations and clustering effects dominate the system dynamics [29], and global order prevails even in the thermodynamic limit [30].

Finally, a compelling biological application of our framework may be found in the vertebrate segmentation clock, where global coupling provides a useful effective description of the system because of the high mobility of cells [31]: by precluding the appearance of local defects, mobility promotes global synchronization. Moreover, it has been recently shown that mobility decreases the relaxation times to achieve synchronization in a model of the segmentation clock that allows for flipping between neighboring cells [32]. However, this system also hosts spatial patterns [33], and mobility is not accounted for in current distributed models. It will be interesting to see how mobility affects the synchrony recovery times and pattern reorganization after perturbation in such models.

Acknowledgments

We thank S Ares, H Chaté, M Matías, A C Oates and D Zanette for valuable comments and discussions. FP acknowledges financial support from the French ANR projects Morphoscale and Panurge. LGM acknowledges support from the CONICET, the ANPCyT PICT 876 and the ERC grant 207634 SegClockDyn.

References

[1] Manrubia S C, Mikhailov A S and Zanette D H 2004 *Emergence of Dynamical Order: Synchronization Phenomena in Complex Systems* 1st edn (Singapore: World Scientific)
[2] Pikovsky A, Rosenblum M and Kurths J 2008 *Synchronization: A Universal Concept in Nonlinear Sciences* (Cambridge: Cambridge University Press)
[3] Strogatz S H 2004 *Sync: How Order Emerges from Chaos in the Universe, Nature, and Daily Life* 1st edn (New York: Hyperion)
[4] Winfree A T 2001 *The Geometry of Biological Time* 2nd edn (Berlin: Springer)
[5] Glass L and Mackey M C 1988 *From Clocks to Chaos: The Rhythms of Life* (Princeton, NJ: Princeton University Press)
[6] Cohen A H, Holmes P J and Rand R H 1982 *J. Math. Biol.* **13** 345
[7] Taylor A F, Tinsley M R, Wang F, Huang Z and Showalter K 2009 *Science* **323** 614
[8] Monte S D, d'Ovidio F, Danø S and Sørensen P G 2007 *Proc. Natl Acad. Sci. USA* **104** 18377
[9] Buscarino A, Fortuna L, Frasca M and Rizzo A 2006 *Chaos* **16** 015116
[10] Tinsley M R, Taylor A F, Huang Z and Showalter K 2009 *Phys. Rev. Lett.* **102** 158301
[11] Kerr B, Riley M A, Feldman M W and Bohannan B J M 2002 *Nature* **418** 171
[12] Reichenbach T, Mobilia M and Frey E 2007 *Nature* **448** 1046
[13] Reichenbach T, Mobilia M and Frey E 2007 *Phys. Rev. Lett.* **99** 238105
[14] Shiogai Y and Kuramoto Y 2003 *Prog. Theor. Phys. Suppl.* **150** 435
[15] Kuramoto Y, Shima S, Battogtokh D and Shiogai Y 2006 *Prog. Theor. Phys. Suppl.* **161** 127
[16] Wiley D A, Strogatz S H and Girvan M 2006 *Chaos* **16** 015103
[17] Sakaguchi H 1988 *Prog. Theor. Phys.* **79** 39
[18] Kuramoto Y 1984 *Chemical Oscillations, Waves, and Turbulence* (Berlin: Springer)
[19] Hildebrand E J, Buice M A and Chow C C 2007 *Phys. Rev. Lett.* **98** 054101
[20] Strogatz S H and Mirollo R E 1991 *J. Stat. Phys.* **63** 613
[21] von Mises R 1918 *Phys. Z.* **19** 490
[22] Mermin N D and Wagner H 1966 *Phys. Rev. Lett.* **17** 1133
[23] Skufca J D and Bollt E M 2004 *Math. Biosci. Eng.* **1** 347
[24] Kosterlitz J M and Thouless D J 1973 *J. Phys. C: Solid State Phys.* **6** 1181
[25] Frasca M, Buscarino A, Rizzo A, Fortuna L and Boccaletti S 2008 *Phys. Rev. Lett.* **100** 044102
[26] Nugent C R, Quarles W M and Solomon T H 2004 *Phys. Rev. Lett.* **93** 218301
[27] Zhou C and Kurths J 2005 *New J. Phys.* **7** 18
[28] Peruani F, Deutsch A and Bär M 2008 *Eur. Phys. J. Spec. Top.* **157** 111
[29] Zanette D H and Mikhailov A S 2004 *Physica* D **197** 203
[30] Toner J, Tu Y and Ramaswamy S 2005 *Ann. Phys.* **318** 170
[31] Riedel-Kruse I H, Müller C and Oates A C 2007 *Science* **317** 1911
[32] Uriu K, Morishita Y and Iwasa Y 2010 *Proc. Natl Acad. Sci. USA* **107** 4979
[33] Morelli L G, Ares S, Herrgen L, Schröter C, Jülicher F and Oates A C 2009 *HFSP J.* **3** 55